DOI: https://doi.org/10.15407/techned2026.03.003

PROTECTION OF ELECTRICAL CONSUMERS AGAINST MICROSECOND HIGH-VOLTAGE SURGES UNDER PARTIAL LOAD OPERATION

V.O. Pavlovskyi[1*], P.Yu. Herasymenko[1], V.K. Gurin[1***], O.M. Yurchenko[1****], D.D. Muhenov[2*****]**
[1] Institute of Electrodynamics National Academy of Sciences of Ukraine,
56, Beresteiskyi Ave., Kyiv, 03057, Ukraine,
E-mail: yuon@ied.org.ua.
[2] National Technical University of Ukraine "Igor Sikorsky Kyiv Polytechnic Institute",
37, Beresteiskyi Ave., Kyiv, 03056, Ukraine.

The paper considers features of consumer protection against microsecond high-voltage surges from the power grid under consumer's partial load operation. A typical protection circuit containing a cascade-connected voltage limiter and a two-stage LC low-pass filter (LPF) is analyzed. Theoretical calculations and simulation studies of the response of the L-shaped LPF to an input voltage surge under the partial load operation of the electrical consumer were carried out, which showed an increase in the response amplitude. To reduce the response of the LPF, it is proposed to introduce resistors in series with each capacitor of the LPF. The results of simulation and experimental verification confirmed the effectiveness of the proposed addition – the maximum voltage surge at the consumer's AC input decreased by up to 2 times. References 17, figures 12.
Key words: microsecond high-voltage surge, immunity, varistor, suppressor.

Introduction. The immunity of radio-electronic and electrical equipment to the action of microsecond high-voltage surge pulses and nanosecond electrical fast transients from the power grid is an important indicator of the reliability and quality of the above-mentioned equipment, which is regulated by international standards on electromagnetic compatibility [1, 2].

High-voltage surges have large destroying ability and are very dangerous for responsible electrical consumers. They occur as a result of power grid failures or as a result of thunderstorm activity [3]. They can also be caused by deliberate actions (so-called "electro-magnetic terrorism" [4]). Another cause of the above-mentioned voltage surges in the power grid is a powerful electromagnetic pulse radiation that occurs in the atmosphere after a nuclear explosion [5].

The difficulty in reducing the amplitude of the residual surge pulse at the consumer's AC input to a level at which the equipment "does not feel" the effect of the surge is that its amplitude can reach 4 kV or more, and the duration of its rise time is in the range of several microseconds [1]. Therefore, in recent decades, significant attention in scientific publications has been paid to this issue [6–9]. Thus, modern transistor-based power converters [10, 11], without dedicated input protection networks against such high-energy surge pulses, are highly susceptible to malfunction or even catastrophic failure.

In [3, 9, 12–14] it is shown that an effective solution of limiting the surge amplitude are two-pole devices with a nonlinear volt-ampere characteristic: varistors, suppressors and gas-filled arresters; they are typically installed at the AC input of the equipment. Each of these means has certain disadvantages: for gas-filled arresters, this is the inertia of operation; for varistors and suppressors, this is a high residual level of the surge (500…900 V) at the output of the amplitude limitation circuit.

To further reduce the amplitude of the surge in [5] it is proposed to include an *LC* low-pass filter (*LC*-LPF) between the surge amplitude limiter and the consumer's AC input, and in [15] a device for protecting a

ORCID: * https://orcid.org/0000-0001-5768-101X; ** https://orcid.org/0000-0001-6244-1133;
*** https://orcid.org/0000-0003-2541-216X; **** https://orcid.org/0000-0002-2107-2308;
***** https://orcid.org/0000-0001-7780-3416

three-phase consumer against the action of an electromagnetic surge pulse caused by an electromagnetic pulse arising in the atmosphere after a nuclear explosion is described. The device consists of two main functional units: amplitude limiting circuit on varistors and suppressors, and an *LC*-LPF. The amplitude limiting circuit is connected between the power grid and the input of the *LC*-LPF.

In [16], the operation of a voltage limiter was investigated for the case when the source of surge has a low internal impedance at high frequencies. It is shown that using a varistor or suppressor together with an *LR*-link reduces the final amplitude of the surge by 1.5 times compared to a varistor or suppressor alone.

In [17], a theoretical analysis and computer simulation using the PSPICE software of the surge pulse passage through the path "voltage limiter – *LC*-LPF – electrical consumer" was carried out. The analysis confirmed the effectiveness of using of the *LC*-LPF between the output of the amplitude limiter and the consumer's AC input and revealed a direct relationship between the *LC*-LPF cutoff frequency, which is determined by the ratings of its elements, and the amplitude of the residual surge.

It is necessary to note that in works cited above the effectiveness of the *LC*-LPF has been confirmed for the operation under a full load of the consumer and a compliance of consumer's equivalent input impedance (Z_{in}) with LPF's characteristic impedance (Z_c) at a zero-frequency. Here $Z_{in} = U^2_{rtd}/P_{rtd}$, where U_{rtd} is the rated rms AC voltage, P_{rtd} is the rated power of the consumer; $Z_c = \sqrt{L_{LPF} / C_{LPF}}$, L_{LPF}, C_{LPF} are the inductance and the capacitance of the *L*-shaped *LC*-LPF link components, respectively.

However, in practice, there is often a situation when the actual power P_{act} of the consumer is less than P_{rtd}, i.e. Z_{in} is greater than Z_c. This means that the *LC*-LPF operates in an out-of-match mode and this may cause an increase in the residual voltage surge at the consumer's AC input caused by the action of the surge. Therefore, it is important to investigate the response of the *LC*-LPF to an input surge under partial load conditions ($Z_{in} > Z_c$).

The purpose of this paper is to improve the scheme for protecting the electrical consumer against large-amplitude pulses in the microsecond range from the power supply network, in particular for the case when the consumer operates in the light load mode.

Mathematical analysis of the *LC*-LPF Response to a Single Input Voltage Jump 1(*t*). Let's consider the response of the *L*-shaped *LC*-LPF (Fig. 1) to a single jump of the input voltage u_{in} (Fig. 2) with a zero edge and an amplitude U_m can be described as:

$$u_{in}(t) = \begin{cases} 0, t < 0; \\ 1, t \geq 0. \end{cases} \tag{1}$$

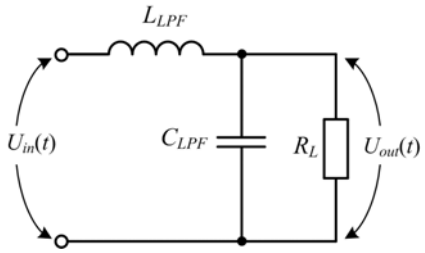

Fig. 1

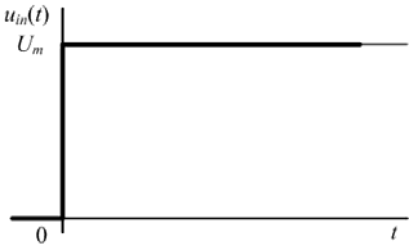

Fig. 2

In the Laplace-domain the voltage transfer function $K(s)$ of the circuit in Fig. 1 can be expressed as follows:

$$K(s) = \frac{1}{s^2 L_{LPF} C_{LPF} + s\dfrac{L_{LPF}}{R_L} + 1}. \tag{2}$$

Denote

$$Z_{in} = \frac{\sqrt{\dfrac{L_{LPF}}{C_{LPF}}}}{r_{pwr}}, \qquad \Omega_c = \frac{1}{\sqrt{L_{LPF} C_{LPF}}}, \tag{3}$$

where Ω_c is the angular frequency of series connected L_{LPF} and C_{LPF}, and r_{pwr} is the coefficient that shows the ratio between P_{act} and P_{rtd} ($P_{act} \leq P_{rtd}$), given by

$$r_{pwr} = P_{act} \Big/ P_{rtd} \,. \tag{4}$$

Considering (3), (2) can be rewritten as:

$$K(s) = \frac{\Omega_c^2}{s^2 + r_{pwr}\Omega_c s + \Omega_c^2}. \tag{5}$$

Four practically important values of r_{pwr} (0.1, 0.2, 0.5, and 1) are considered in the following analysis. The output voltage $U_{out}(s)$ of the *LC*-LPF in the Laplace-domain is given by:

$$U_{out}(s) = U_{in}(s) \cdot K(s) \tag{6}$$

where $U_{in}(s)$ is the input voltage in the Laplace-domain. Then the input voltage is a single voltage jump 1(t) (Fig. 2), which in Laplace-domain is defined as:

$$U_{in}(s) = U_m / s \,. \tag{7}$$

The denominator (7) has three roots:

$$s_1 = 0, s_{2,3} = -\frac{\Omega_c}{2}\left(r_{pwr} \pm \sqrt{r_{pwr}^2 - 4}\right). \tag{8}$$

Considering that $r_{pwr} \le 1$, $S_{2,3}$ are complex conjugate, and they can be represented as follows:

$$s_1 = 0, s_{2,3} = -\frac{\Omega_c}{2}\left(r_{pwr} \pm \sqrt{r_{pwr}^2 - 4}\right). \tag{9}$$

With these roots, u_{out} in the time domain can be defined as:

$$\begin{gathered} u_{out}(t) = U_m + 2\,\mathrm{Re}\left(\frac{2U_m}{r_{pwr}^2 - 4 - jr_{pwr}\sqrt{4 - r_{pwr}^2}} e^{-\frac{r_{pwr}\Omega_c}{2}\left(1 - j\frac{\sqrt{4 - r_{pwr}^2}}{r_{pwr}}\right)t} \right) = \\ U_m \left\langle 1 - e^{-\frac{\Omega_c r_{pwr}}{2}t} \cdot \left\{ \cos\left[\left(\frac{\Omega_c}{2}\sqrt{4 - r_{pwr}^2}\right)t\right] + \frac{r_{pwr}}{\sqrt{4 - r_{pwr}^2}} \cdot \sin\left[\left(\frac{\Omega_c}{2}\sqrt{4 - r_{pwr}^2}\right)t\right] \right\} \right\rangle. \end{gathered} \tag{10}$$

Equation (6) can be as represented as follows:

$$U_{out}(s) = \frac{U_m \Omega_c^2}{s(s^2 + r_{pwr}\Omega_c s + \Omega_c^2)} \,. \tag{11}$$

Equation (11) yields the following time-domain expression for the output voltage u_{out}:

$$u_{out}(t) = U_m \left\langle 1 - e^{-\frac{\Omega_c r_{pwr}}{2}t} \cdot \left\{ \cos\left[\left(\frac{\Omega_c}{2}\sqrt{4 - r_{pwr}^2}\right)t\right] + \frac{r_{pwr}}{\sqrt{4 - r_{pwr}^2}} \cdot \sin\left[\left(\frac{\Omega_c}{2}\sqrt{4 - r_{pwr}^2}\right)t\right] \right\} \right\rangle. \tag{12}$$

Fig. 3 shows the result of calculating u_{out} according to (9) for the four values of r_{pwr} mentioned above. For the calculation, following parameters of the *LC*-LPF were used: L_{LPF} = 1.6 mH, C_{LPF} = 16 uF, Z_{in} = 10 Ohm for r_{pwr} = 1; U_m = 1 V.

As it can be seen from waveforms of u_{out} in Fig. 3, with a decrease in the value of r_{pwr} the peak value of u_{out} increases and the total duration of the transient process at the output of the *LC*-LPF increases as well. It can also be seen from the above curves that the peak value at r_{pwr} = 0.1 is much higher than its steady-state value, which can have extremely negative consequences for the consumer, up to its failure.

Simulation of the *LC*- and *RLC*–LPFs Response to the Single Input Voltage Jump 1(*t*). To verify the validity of (12), the response of the *LC*-LPF to the input voltage jump 1(t) was modeled using PSPICE.

The simulation results are shown in Fig. 4. Response of the *LC*-LPF to the input voltage jump 1(*t*) obtained from simulation.

Comparison of the calculation and simulation results shows a deviation of no more than 1%, which confirms the reliability of (12).

As it can be seen from waveforms of u_{out} in Figs. 3 and 4, it is clear that the output voltage's peak value and the duration of the transient process increase with decreasing r_{pwr}. Thus, for r_{pwr} = 1 the voltage peak value of the largest surge is less than 20% of the steady-state value, and for r_{pwr} = 0.1 the above-mentioned peak value exceeds the steady-state value by almost 2 times.

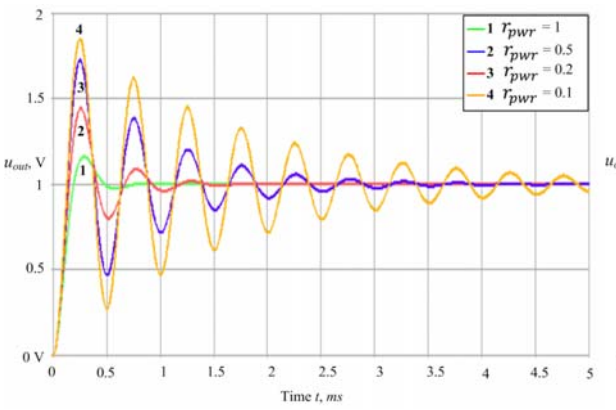

Fig. 3

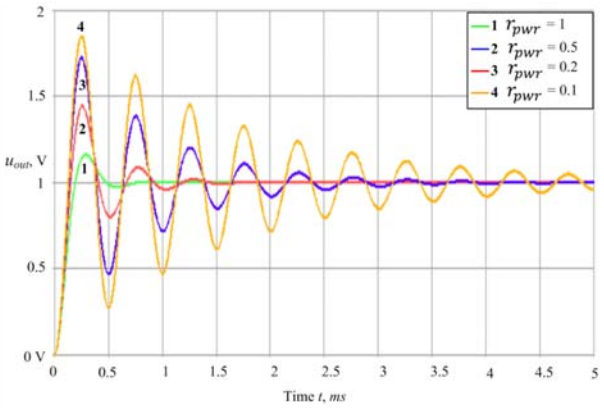

Fig. 4

To reduce the largest voltage's peak value, it is proposed to supplement the *LC*-LPF circuit with a resistor R_c, which is connected in series with the capacitor C_{LPF} (Fig. 5).

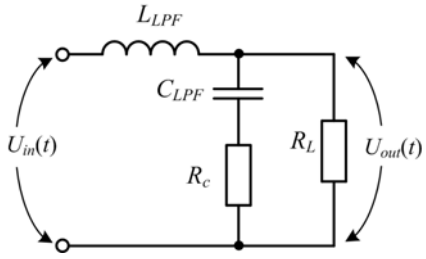

Fig. 5

Simulation results show a positive effect of such solution, i.e. a reduction both the largest voltage's peak value and the duration of the transient process, provided that $R_c \geq Z_c = \sqrt{L_{LPF} / C_{LPF}}$. Fig. 6 shows waveforms of u_{out} for the *RLC*-LPF and four values of R_c: 0.1 Ohm, 10 Ohm, 20 Ohm, 30 Ohm in the case of $Z_{in} = 10Z_c = 100$ Ohm ($r_{pwr} = 0.1$).

As it can be seen from Fig. 6, there is a significant decrease in the peak-value of the voltage surge and a significant decrease in the duration of the transient process with increasing R_c value. Thus, for R_c = 30 Ohms, the largest voltage's peak value decreases by more than 40 times.

Experimental Results. Experimental studies were carried out with a mock-up of an *L*-shaped *RLC*-LPF. The measurement scheme is shown in Fig. 7. The inductance L_{LPF} = 1.6 mH, the capacitance C_{LPF} = 16.8 uF realized by connecting three EPCOS B23924 capacitors (5.6 uF, X2, 305 VAC) in parallel. The choke L_{LPF} is wound on four Magnetics 0077192A7 toroidal cores with 56 turns. The MOSFET IPP034NE7N3 (V_{ds} = 75 V, I_{ds} = 100 A) is used as the switch S_1. The voltage rise rate after S_1 to the input voltage level U_{in} = 10 VDC with an active load of 1 kOhm was 70 ns.

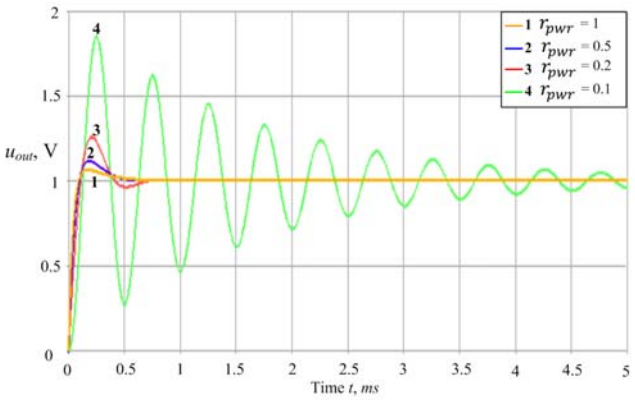

Fig. 6

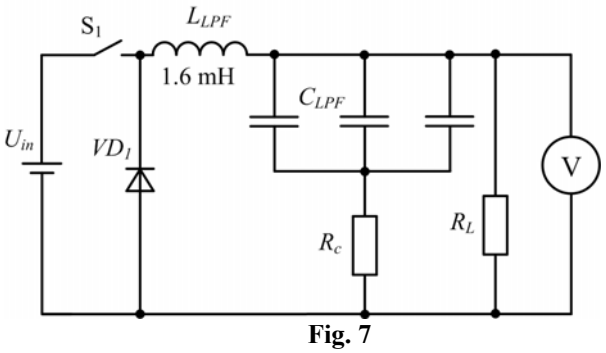

Fig. 7

Fig. 8 shows waveforms of u_{out} obtained during measurements: (*a*) R_c = 0.1 Ohm; (*b*) R_c = 30 Ohm. Waveforms of u_{out} under R_L = 100 Ohm are shown in Fig. 8, *a* and for R_c=30 Ohm – in Fig. 8, *b*. Comparison of the waveforms in Fig. 8 with the corresponding ones in Fig. 6 for R_c = 0.1 Ohm and R_c = 30 Ohm shows that they are practically the same, which confirms the reliability of the simulation results.

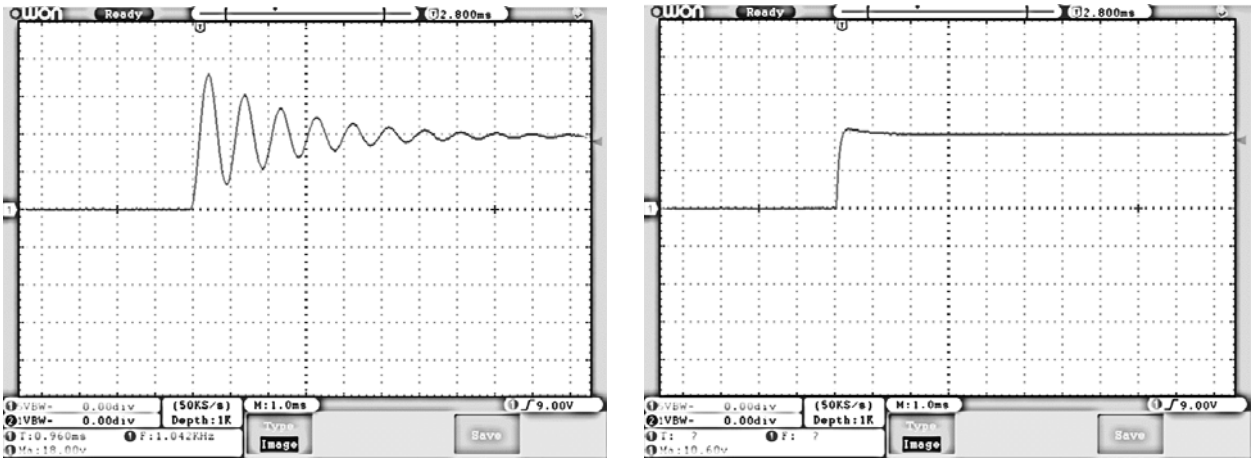

a *b*

Fig. 8

Standardized surge pulse and its applying to the device under test. According to the requirements [1], a standardized high-energy surge pulse from a 1.2/50 combination wave generator (CWG) enters to the AC input of the device under test (DUT) through a capacitor of 18 uF. The amplitude of the standardized surge pulse is selected from the range 0.5 kV; 1 kV; 2 kV; 4 kV depending on the given degree of test severity. The circuit to supply a surge pulse from the CWG to the AC input of the DUT, and a decoupling device, which does not allow the standardized surge, pulse to penetrate into the common AC power grid, shown in Fig. 9.

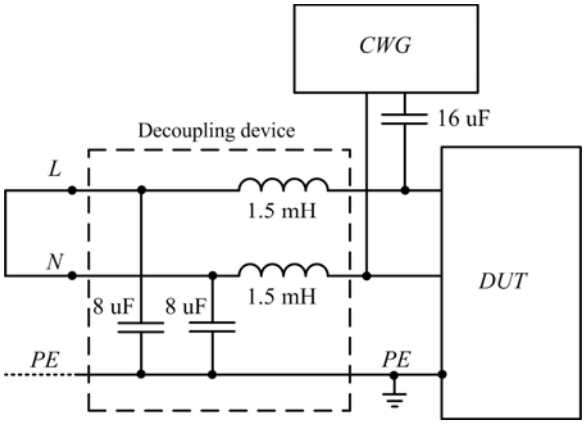

Fig. 9

For generation of a surge pulse, a CWG unit was manufactured in accordance with the recommendations of the standard [1]. In the case of the open-circuit mode, the realized duration of the CWG's surge pulse rise was 1.3 us, while the half amplitude duration was 52 us, and the pulse amplitude at the generator output was 500 V. In the case of the short-circuit mode, the duration of the current pulse rise was 7 us, the duration of the current pulse at half the amplitude was 18 μs, and the amplitude of the current pulse was 260 A. Thus, according to the rules for calculating the output resistance of the CWG given in the above-mentioned standard [1], the internal resistance R_i of the CWG unit was 500/260 ≈ 1.92 Ohm, which meets the requirement of $R_c \leq 2$ Ohm.

To simplify measurements and analysis of u_{out} under the action of a pulse from the CWG, the pulse was applied to the DUT input with the "*L*" and "*N*" conductors shorted and disconnected from the power grid (Fig. 9).

As a DUT, a typical scheme presented in [13] for protecting the electrical consumer from the action of high-energy high-voltage surge pulse from the power grid was used. The DUT sample, shown in Fig. 10, *a*, contains a voltage limiter based on the varistor combined with the *LR* chain [14], and a two-stage LPF. The complete DUT circuit is shown in Fig. 10, *b*.

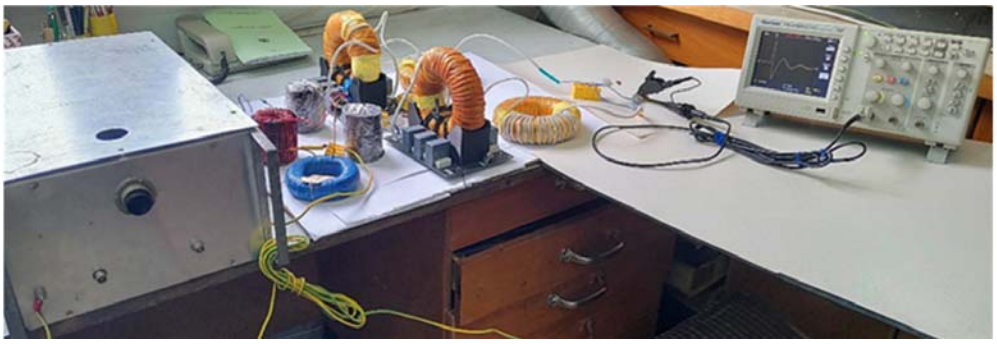

a

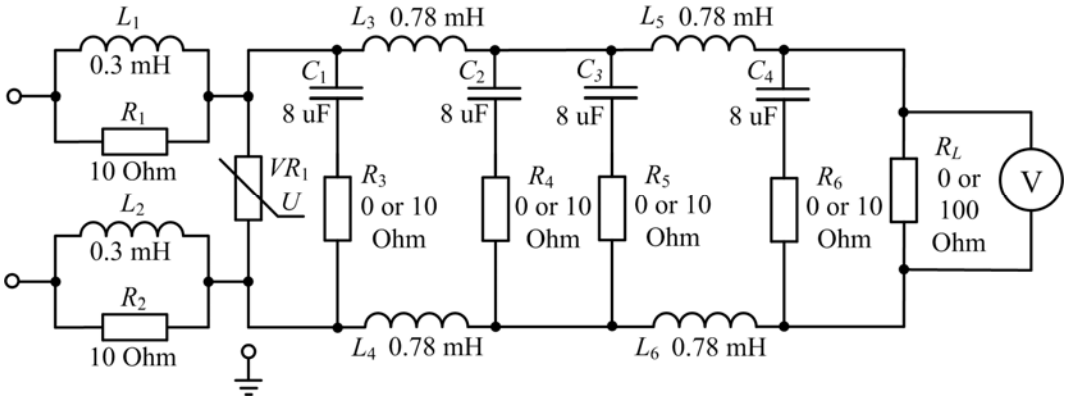

b

Fig. 10

Each of the capacitors $C_1..C_4$ in the scheme of Fig. 10, *b* consists of four polypropylene capacitors MKP-X2 of 2 uF, 310VAC, connected in parallel. The inductance of the air core Inductors L_1 and L_2 is 0.3 mH. Chokes $L_3…L_6$ are wound on Magnetics 0077192A7 toroidal cores, their inductance is 0.78 mH. The value of Z_c of the two-stage LPF is 10 Ohm at the zero-frequency (f = 0), the resistance of resistors $R_1…R_6$ is 10 Ohm, R_L = 10 Ohm for the case of r_{pwr} = 1, and R_L = 100 Ohm for the case of r_{pwr} = 0.1. The voltage limiter uses a 20D361K varistor VR_1.

Fig. 11 shows the waveforms of u_{out} for R_L = 100 Ohm, and the amplitude U_m^{srg} of the surge pulse U_m^{srg} = 500 V, for two cases: 1) R_3...R_6 are shorted ($R_3 = R_4 = R_5 = R_6 = 0$); 2) $R_3 = R_4 = R_5 = R_6 = Z_c$ = 10 Ohm.

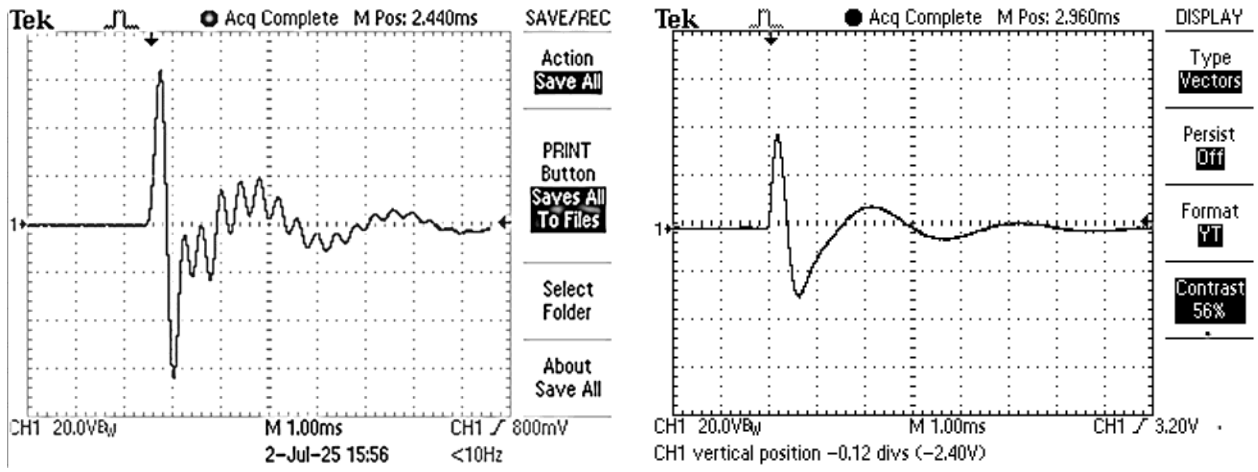

a *b*

Fig. 11

Waveforms of residual voltage at the LPF output, R_L = 100 Ohm for case 1 are shown in Fig. 11, *a* and for case 2 – in Fig.11, *b*. As can be seen from these waveforms, introducing resistors in series with each LPF capacitor reduces the largest voltage peak value on R_L from 64 V to 40 V, i.e. by 1.6 times.

To make sure that the incorporation of the above-mentioned resistors in series with the LPF capacitors does not impair the operation of the device in the nominal load mode, Fig. 12 shows the voltage waveforms across the resistor R_L = 10 Ohm, for the same cases.

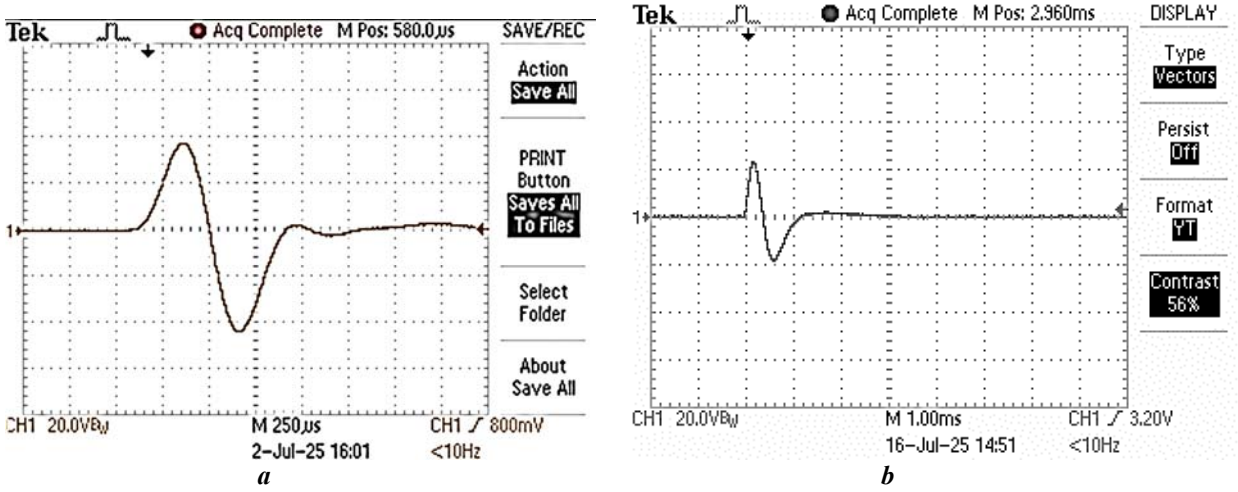

a *b*

Fig. 12

Waveforms of residual voltage at the LPF output, R_L = 10 Ohm for case 1 are shown in Fig. 12, *a* and for case 2 – in Fig. 12, *b*. As can be seen from these waveforms, introducing resistors in series with each LPF capacitor in the rated load mode also reduces the largest voltage peak value on R_L from 42 V to 23 V, i.e. almost twice.

Thus, experimental studies of the DUT mock-up's response to the action of a standardized surge pulse confirmed the results of theoretical analysis and computer simulation.

Conclusions. Theoretical analysis and computer modeling have shown that improvement of the circuit for protecting the consumer from large-amplitude overvoltage pulses in the microsecond range from the power supply network by introducing resistors in series with *LC*-LPF capacitors of the protection circuit significantly reduces the amplitude of the overvoltage pulse at the consumer's power input in both light and nominal load modes. The resistance of the resistors added to the protection circuit must be commensurate with the characteristic impedance of the *LC*-LPF at zero frequency.

Experimental studies of the response of an improved protection circuit's model to the action of a pulse from a microsecond pulse interference generator (according to the standard IEC 61000-4-5) confirmed the results of theoretical analysis and computer modeling. The introduction of the mentioned resistors reduces the amplitude of the overvoltage pulse at the consumer's mains input by 1.6 times for the light mode (100% consumer power), compared to a typical protection scheme.

1. EN 61000-4-5:2014/A1:2017. Electromagnetic compatibility (EMC). Part 4-5: *Testing and measurement techniques. Surge immunity test*. 2017.

2. EN 61000-4-4:2012 Electromagnetic compatibility (EMC). Part 4-4: *Testing and measurement techniques. Electrical fast transient/burst immunity test*. 2012.

3. Ott H.W. Electromagnetic Compatibility Engineering. New Jersey: John Wiley & Sons, Inc., 2009. 843 p. DOI: https://doi.org/10.1002/9780470508510.

4. Gurevich V. Electromagnetic Terrorism: New Hazards. *Electrical Engineering and Electromechanics.* 2005. No 4. Pp. 81-83.

5. Ricketts L.W., Bridges J.E., Myletta J. Electromagnetic pulse and protection methods. Moskva: Atomizdat, 1979. 328 p. (Rus).

6. Tao Liang., Yan-zhao Xie. Maximizing Radiated High-Power Electromagnetic Threat to Transmission Line System Under the Constraints of Bounded Bandwidth and Amplitude. *IEEE Transactions on Electromagnetic Compatibility*. 2021. Vol. 63. Issue 3. Pp. 840-847. DOI: https://doi.org/10.1109/TEMC.2020.3040271.

7. William A.R., Richard H. Recent Developments in High Power EM (HPEM) Standards With Emphasis on High Altitude Electromagnetic Pulse (HEMP) and Intentional Electromagnetic Interference (IEMI). *IEEE Letters on Electromagnetic Compatibility Practice and Applications*. 2020. Vol. 2. Issue 3. Pp. 62-66. DOI: https://doi.org/10.1109/LEMCPA.2020.3009236.

8. Marian L., Michael S., Holger H. HPEM - Based Risk Assessment of Substations Enabled for the Smart Grid. *IEEE Transactions on Electromagnetic Compatibility*. 2020. Vol. 62. Issue 1. Pp. 173-185. DOI: https://doi.org/10.1109/TEMC.2019.2893937.
9. Giri D.V., Hoad R., Sabath F. Implications of high-power electromagnetic (HPEM) environments on electronics. *IEEE Electromagnetic Compatibility Magazine*. 2020. Vol. 9. Issue 2. Pp. 37-44. DOI: https://doi.org/10.1109/MEMC.2020.9133238.
10. Martynov D.V., Rudenko Yu.V., Martynov V.V. Research of a bidirectional converter using an asymmetric inverter with a magnetically coupled two-winding inductor in an energy storage system. *Tekhnichna Elektrodynamika*. 2025. No 3. Pp. 15-21. DOI: https://doi.org/10.15407/techned2025.03.015. (Ukr).
11. Martynov D.V., Rudenko Yu.V., Martynov V.V. Improving the operation of an asymmetric inverter with magnetically coupled inductors for energy storage systems. *Electrical Engineering & Electromechanics*. 2025. No 4. Pp. 53-58. DOI: https://doi.org/10.20998/2074-272X.2025.4.07.
12. Ozenbauch R.L., Pullen T.M. EMI Filter Design. CRC Press, 2001. 348 p. DOI: https://doi.org/10.1201/9780203910313.
13. Tihanyi L. Electromagnetic Compatibility in Power Electronics. IEEE Press, 1995. 403 p.
14. Kularatna N., Ross A.S., Fernando J., James S. Design of Transient Protection Systems. Elsevier Inc., 2018. 282 p.
15. Liu Dejun, Wu Fei. Nuclear electromagnetic pulse protection device. Patent USA No CN118352980(A), 2024.
16. Pavlovskyi V.O., Gurin V.K., Yurchenko O.M. Increasing of electrical and radioelectronic equipment immunity against high voltage short-duration pulse disturbances in the mains. *Tekhnichna Elektrodynamika*. 2022. No 5. Pp. 34-37. DOI: https://doi.org/10.15407/techned2022.05.034. (Ukr).
17. Pavlovskyi V.O., Gurin, V.K., Yurchenko, O.M. Analysis of electromagnetic processes in the "voltage limiter-low-frequency filter" circuit during the influence of high-voltage surge from the power supply network. *Tekhnichna Elektrodynamika*. 2023. No 4. Pp. 37-42. DOI: https://doi.org/10.15407/techned2023.04.037. (Ukr).

УДК 621.391

ЗАХИСТ ЕЛЕКТРОСПОЖИВАЧІВ ВІД ВИСОКОВОЛЬТНИХ ІМПУЛЬСНИХ ЗАВАД МІКРОСЕКУНДНОГО ДІАПАЗОНУ ТРИВАЛОСТЕЙ У ПОЛЕГШЕНОМУ РЕЖИМІ НАВАНТАЖЕННЯ

В.О. Павловський[1], канд. техн. наук, **П.Ю. Герасименко**[1], канд. техн. наук,
В.К. Гурін[1], канд. техн. наук, **О.М. Юрченко**[1], докт. техн. наук, **Д.Д. Мугенов**[2]
[1] **Інститут електродинаміки НАН України,**
пр. Берестейський, 56, Київ, 03057, Україна.
E-mail: yuon@ied.org.ua.
[2] **НТУ України "Київський політехнічний інститут ім. Ігоря Сікорського",**
пр. Берестейський, 37, Київ, 03056, Україна.

У роботі розглянуто особливості захисту електроспоживачів від високовольтних імпульсних завад мікросекундного діапазону тривалостей (МІП) у полегшеному режимі навантаження. Проведено аналіз типової схеми захисту, яка складається з каскадно з'єднаних схем обмежувача амплітуди і двокаскадного фільтра нижніх частот (ФНЧ). Проведено теоретичні розрахунки і моделювання відгуку Г-подібної ланки ФНЧ на дію МІП для режиму полегшеного навантаження, які показали збільшення амплітуди залишкової напруги МІП на виході ланки. Задля зменшення амплітуди відгуку запропоновано включити резистори послідовно з кожним конденсатором ФНЧ. Результати моделювання та експериментальні дослідження підтвердили ефективність запропонованого технічного рішення – максимальна амплітуда залишкової напруги МІП на електромережному вході електроспоживача зменшилася майже вдвічі. Бібл. 17, рис. 12.

Ключові слова: високовольтні імпульсні завади, захищеність апаратури, варистор, супресор.

Received 27.10.2025
Accepted 16.02.2026